Iranian Journal of Chemical Engineering

Journal Homepage: www.ijche.com

pISSN: 1735-5397
eISSN: 2008-2355

Regular Article

Improving the Performance of a Two-Phase Ejector Using the Genetic Algorithm Based on the Secondary Fluid Entrainment Rate

M. Moghaddasi [1], ***M. Keshavarz Moraveji*** [2*], ***O. Alizadeh*** [3]

[1] *Department of Chemical Engineering, Borujerd Branch, Islamic Azad University, Borujerd, Iran*
[2] *Department of Chemical Engineering, Amirkabir University of Technology (Tehran Polytechnic), Tehran, Iran*
[3] *Department of Chemistry and Chemical Engineering, Rasht Branch, Islamic Azad University, Rasht, Iran*

ARTICLE INFO

Article history:
Received: 2023-03-28
Accepted: 2023-05-13
Available online: 2023-05-21

Keywords:
Entrainment Rate of the Secondary Fluid,
Gas-Liquid Ejector,
Recovery of the Flare Gas,
Geometry Design,
Multi-Objective Genetic Algorithm Uptimization,
Computational Fluid Dynamics

ABSTRACT

Ejectors offer a cost-effective and practical solution for recovering flare gases, thereby reduce greenhouse gases. Improving the entrainment rate of the secondary fluid can enhance the performance of ejectors. The objective of this research is to identify the optimal geometry of the ejector to maximize the absorption rate of the secondary fluid. Computational fluid dynamics are used to evaluate a two-phase ejector. The geometric parameters such as the diameter and length of the throat, nozzle diameter, and converging and diverging angles impact the absorption rate of the secondary fluid. By using a multi-objective genetic algorithm, the optimal values for all parameters are obtained. The results show that reducing the length and angle of the throat of the converging section, as well as the nozzle diameter, leads to increased absorption. In contrast, the throat diameters and angle of the divergent section increase absorption. Additionally, the energy efficiency is investigated in basic and optimized geometries. The findings reveal that increasing the soak range does not necessarily enhance the energy efficiency.

DOI: 10.22034/ijche.2023.390350.1488 URL: https://www.ijche.com/article_171527.html

1. Introduction

The term "flaring" encompasses two concepts: (a) the combustion of flammable gases from equipment and parts removed from various oil and gas refineries and petrochemical complexes, and (b) the continued burning of gas instead of its recovery. The flaring system is responsible for emitting the largest quantity of environmental pollutants [1, 2].

Researchers have proposed different methods and techniques to reduce and recover the gases sent to the flare. Some authors have

*Corresponding author: moraveji@aut.ac.ir (M. Keshavarz Moraveji)

dedicated their focus to modifying production in general, i.e., gas production units in particular, to reduce the amount of gases transferred to the flare [3, 4]. Recovering flare gases is another approach to the reduction of the greenhouse gas emission [5-13]. The use of certain systems for the gas compression can reduce the flaring rate. Therefore, gases can be collected and recovered.

It is of note that the application of an ejector is one way among many to recover the flare gas. Leagas et al. [14] focused on the cost-effectiveness and efficiency of the ejector technology for recovering the flare gas. Ainge [15] demonstrated that a compressor could best be used as an efficient technique to recover the flare gas. The author discussed the use of the ejector technology as an alternative to the rotary-type compression equipment. Mazumder et al. [16] presented a new approach that involved combining the ejector-based flare gas recovery method with the developed thermal vapor compression method. Eshaghi and Hamrang [17] utilized the gas-gas ejector as an alternative to the compressor. Bashiri et al. [18] designed a syngas purification system derived from integrated biomass with certain modifications. Ainge and Al-Khateeb [19] reviewed the latest advances in the ejector technology and studied its use as a compressor for the flare gas recovery. Researchers have used the ejector in these networks instead of other compressors and examined their cost-effectiveness from a technical point of view. The results suggest that utilizing ejectors for recycling the flare gas can provide economic benefits and energy savings. Nevertheless, researchers have not extensively investigated the influence of the ejector's geometrical parameters on its performance.

Ejectors are widely used in the chemical industry for the suction, compression, transfer, or mixing of both fluids and solid particles [20-25]. Depending on requirements and demands, there are different ways to design and optimize ejectors. One way is to increase the entrainment rate of the secondary fluid, referred to as the intensity of the mixture of two substances, or the transfer of fluid from a low-pressure area to a high-pressure area. The most important objective of this research is to increase the entrainment rate of the recovery gas.

Initially, the performance of ejectors is analyzed based on one-dimensional classical gas dynamics. Subsequently, this theory was further modified to incorporate the loss coefficients in the mixing chamber, nozzle, and diffuser. However, the geometry of the ejector remained unchanged in this analysis [26]. The development of numerical methods has encouraged researchers to utilize methods that involve computational fluid dynamics. Researchers utilized the computational fluid dynamics (CFD) method to study the flow in ejectors and optimize their performance. Sriveerakul et al. [26] studied the effects of the functional conditions and geometrical properties of ejectors on their performance. Yadav and Patwardhan [27] optimized the geometry of the ejector suction chamber using the computational fluid dynamics method. Galanis and Sorin [20] presented a one-dimensional thermodynamic model to investigate the behavior of ejectors and determine the highest possible compression ratio for the given inlet conditions, mass flow rate, and suction fluids. Wang et al. [21] employed CFD to optimize the primary geometry of the nozzle and showed that the performance of the ejector was highly dependent on the length and angle of the divergence. However, their findings only

focused on optimizing the geometry of the nozzle section. Suvarnakuta et al. [23] employed computational fluid dynamics to investigate the performance of a steam ejector in refrigeration systems and to enhance the operational flexibility and coefficient of the performance.

After reviewing past research, the following points caught our attention:

- ✓ One-dimensional mathematics was conducted in past research to model ejectors.
- ✓ The efficiency of steam ejectors in refrigeration systems was optimized in past studies that were limited to specific operating conditions.
- ✓ Past research merely investigated the specific parts of the geometry of the ejector, such as the suction part.
- ✓ The technical and economic effects of using ejectors instead of other compressors in the recovery of the flare gas were investigated.

The current research investigates the use of gas-liquid ejectors in the recovery of the flare gas through computational fluid dynamics simulations. We optimized the diameter and length of the throat, as well as the diameter and angles of the nozzle (convergent and divergent) using a multi-objective genetic algorithm to achieve the maximum entrainment rate of the secondary fluid.

2. Simulation using computational fluid dynamics

In a two-phase (liquid-gas) ejector, a high-velocity liquid enters the ejector through the primary inlet and generates a low-pressure region in the throat. The pressure gradient between the nozzle tip and the inlet section of the secondary fluid causes it to generate the force necessary to absorb the gas (secondary fluid) [27]. Researchers frequently use Euler-Lagrange and Euler-Euler approaches to model two-phase flows. In the second method, all phases are considered continuous [28, 29]. Yadav and Patwardhan [27] proposed an Euler-Eulerian (mixed model) approach to simulate the liquid-gas ejector. The governing equations for transient multiphase flow are as follows [30-33].

The mass conservation equation (continuity) for each phase is given below:

$$\frac{\partial}{\partial t}(\alpha_k \rho_k) + \nabla.(\alpha_k \rho_k u_k) = S_k \tag{1}$$

Conservation of the momentum for each phase:

$$\begin{aligned}\frac{\partial}{\partial t}(\alpha_k \rho_k u_k) + \nabla.(\alpha_k \rho_k u_k u_k) &= -\alpha_k \nabla p_k \\ &+ \nabla.\left(\alpha_k \mu_k \left(\nabla u_k + (\nabla u_k)^T\right)\right) + \alpha_k \rho_k g \\ &+ M_k\end{aligned} \tag{2}$$

where ρ_k, α_k, and u_k represent density, volume fraction, and phase velocity respectively. S_k indicates the rate phase production between different phases. Parameters p_k, μ_k, and g express the pressure, viscosity, and gravitational acceleration of the phase k respectively. M_k is the sum of surface forces including lifting, drag, turbulence dispersion, wall lubrication, and virtual mass. The virtual mass is negligible compared to other forces for multiphase flows under stable conditions [34]. Therefore, in the present work, the effects of this force are neglected.

By considering the continuity and momentum equations for all phases, the mixture momentum conservation is obtained below:

$$\frac{\partial}{\partial t}(\rho_m u_m) + \nabla.(\rho_m u_m u_m) = -\nabla p_m + \nabla.(\mu_m\left(\nabla u_m + (\nabla u_m)^T\right)) + \rho_m g + M_m \quad (3)$$

where the subscript m indicates the quantity related to the mixture. The secondary velocity (s) corresponding to the primary phase (p), also known as the relative velocity or slip to face, is defined [27, 35].

$$u_{sp} = u_s - u_p \quad (4)$$

In this research, the Fluent software is used to simulate the two-phase flow in the ejector. In this software, the sliding speed provided by Manninen et al. [36] is employed here.

$$u_{sp} = \frac{t_s}{F_d}\left(\frac{\rho_s - \rho_m}{\rho_s}\right)\vec{a} \quad (5)$$

The drag force (Fd) can be calculated through the following equation [21, 29].

$$F_d = \begin{cases} 1 + 0.15\,(Re)^{0.687} & Re \le 1000 \\ 0.0183 & Re > 1000 \end{cases} \quad (6)$$

where Re represents the Reynolds number. This equation, which utilizes user-defined functions and is introduced to the Fluent software, takes the form of DEFINE_VECTOR_ EXCHANGE_ PROPERTY.

3. Verification of the results of computational fluid dynamics

To validate the calculation results of the fluid dynamics simulation, the geometry of the experimental model proposed by Bhutada and Pangarkar [37] was selected. In their model, water is the primary phase while air is treated as the secondary fluid. The validation results are for a case where the diameter of the throat and the area of the throat to the nozzle are equal to 16 and 4 mm respectively. The angles of the converging and diverging areas are 12 and 5 degrees respectively. Bhutada and Pangarkar [37] reported that the entrainment rate of the secondary fluid (air) was equal to 0.00294 kg/s under these geometrical conditions.

Due to the axial symmetry of the geometry of the ejector, a two-dimensional axial symmetry model was used. Air (with a diameter of one millimeter) was assumed to be the primary and water was the secondary phase of the ejector. The following boundary conditions were used: (1) The water inlet velocity was set to 21.2 m/s; (2) The relative pressure at the air inlet was set to zero using a pressure gauge; (3) The gauge pressure at the ejector outlet was set to zero; and (4) The non-slip condition was maintained on the walls of both the ejector and the nozzle. "Coupled" models and "PRESTO" were used for pressure-velocity and discrete pressure connections respectively. The second-order upwind model was applied to determine the turbulence kinetic energy, discrete momentum, and turbulence dissipation rate. The under-relaxation coefficient of 0.1 was considered for the pressure, density, momentum, sliding speed, and volume fraction.

Due to the disparity in CFD results, different grid sizes were generated and implemented in the domain. From the grid with a size of 0.25 mm, the results experienced better convergence and less fluctuations. Therefore, this network is used in the following sections of this study. The flow inside the ejectors due to the high Reynolds Number is turbulent. Many studies have adopted different approaches to flow modeling turbulence in two-phase ejectors [23, 26-28, 37-39]. In the

present research, the "Realizable -ε" method was employed to model the turbulent flow.

After performing calculations, it was found that the absorption rate of the secondary fluid (air) was 0.002863 kg/s, which differs from the experimental data of Ref. [37] by 2.6 %. However, this level of error is considered acceptable for numerical results.

4. Multi-objective genetic algorithm

The multi-objective genetic algorithm is a search algorithm that is used to optimize multiple objectives simultaneously. It is a powerful optimization tool that utilizes genetic operators to accurately explore the entire solution space. The Genetic Algorithm identifies the parameters needed to achieve the best results, or optimal mode. The remarkable feature of the Genetic Algorithm is its ability to avoid converging to local optima, thereby finding the overall optimal point in the entire domain. Furthermore, the Genetic Algorithm can optimize more than one parameter in a single problem, as reported in [40].

In the classical genetic algorithm, if a problem has multiple objective functions, the user must evaluate their importance by assigning weights to each of them. However, with the multi-objective genetic algorithm, a new approach is introduced to evaluate candidate parameters without the need to define relative importance coefficients. This provides a more efficient and accurate optimization method for multi-objective problems [40-42].

The candidates in a multi-objective problem are Pareto optimal, meaning that there is a chance of having both local and global optimal scores, just as in a single-objective problem. After the first evaluation of a population, a set of solutions, or candidate points, is classified into different non-dominant levels, creating the initial and best non-dominant set population. This set is evaluated once again, and the non-dominated solutions form the second level, which is the next best. The same method is used again to identify non-dominant solutions of the third level, and this process continues until all members are at a non-dominant level. The minimum state of a non-dominated surface occurs when no solution dominates any other solution, and all candidates of the initial population fall into one category. At most, N non-dominant levels arise when a hierarchy of mastery exists, where any solution is exactly dominated by another level in the set [42].

5. Results and discussion

The primary fluid is the liquid phase, consisting of amine, while the secondary fluid is the gas phase, consisting of the flare gas. Table 1 provides their respective physical properties. As depicted in Figure 1, a specific geometry is considered as the base state.

The problem was modeled using the computational fluid dynamics method in the Fluent software. The absorption rate of the flare gas was calculated to be 0.0024846 kg/s. Figure 2 shows the axial velocity for the flare gas and amine, as well as the turbulence intensity of the mixture in the ejector, as depicted by the lines.

The objective of this study is to achieve an optimal design of the geometry of the ejector and improve the absorption rate of the secondary fluid (the flare gas). The design parameters to be optimized include the length and diameter of the throat, the diameter of the nozzle, the diameter of the liquid inlet, and the converging and diverging section angles, as shown in Figure 3. Target variables (the absorption rate) and the design are parametrically defined in the Fluent software.

Design variables cannot take any arbitrary values. For instance, the radius of the nozzle should not exceed the radius of the inlet. This leads to the creation of a constrained optimization problem, which can be tackled using the investigated multi-objective genetics algorithm.

Table 1
Properties of amine and the flare gas.

	Density (ρ) $[kg/m^3]$	Heat capacity (c_P) $[J/kg \cdot K]$	Thermal conductivity (k) $[W/m \cdot K]$	Viscosity (μ) $[Pa \cdot s]$
Amine	1064	3193	0.2557	0.0103
Flare gas	ideal gas	1978	0.0509	1.228e-5

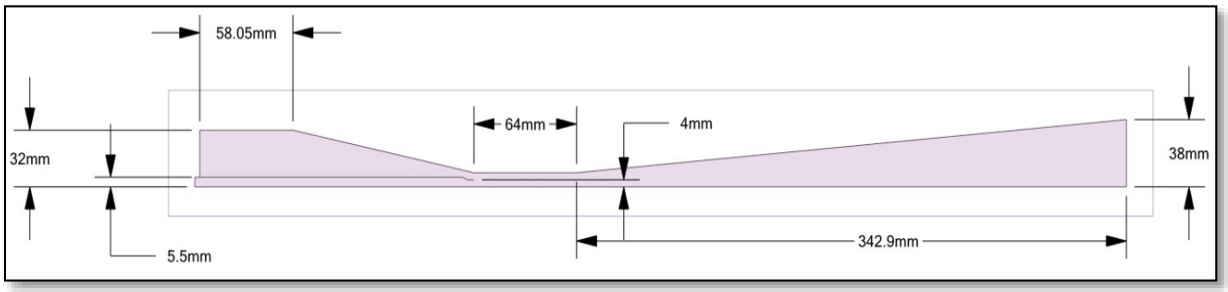

Figure 1. Geometrical parameters of the base case.

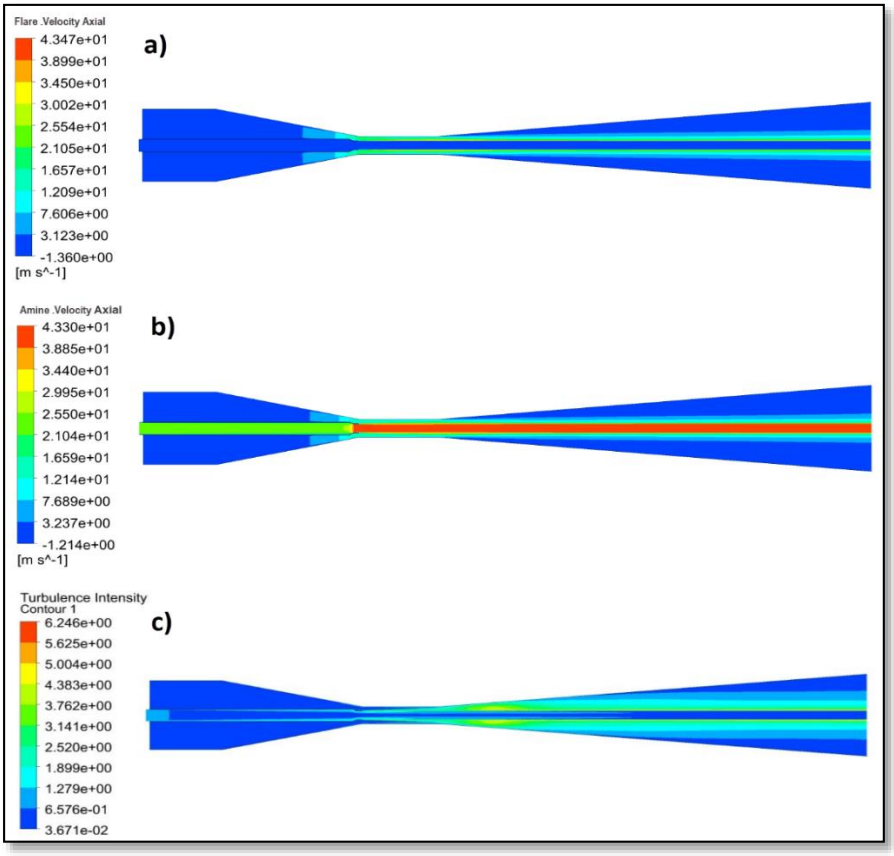

Figure 2. a) Flare gas; b) amine axial velocity contours; and c) the turbulence intensity of the mixture.

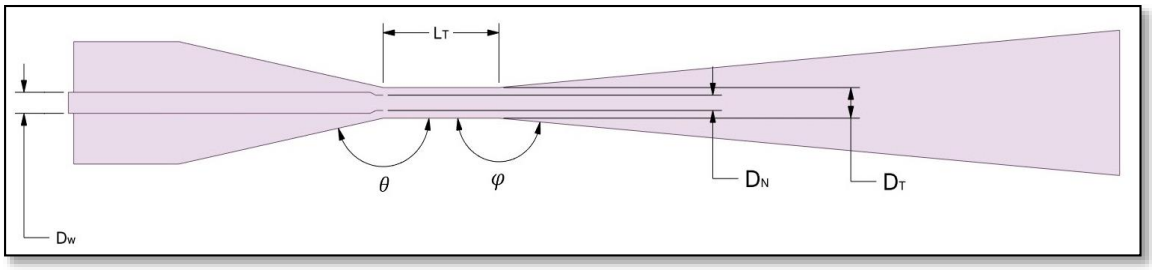

Figure 3. Design parameters of the two-phase ejector.

In meta-heuristic optimization algorithms, an acceptable range of variation should be considered for each design parameter. The researchers have reported values for the geometry of the nozzle and throat, as well as the converging and diverging angles, in which the absorption rate is maximum. Based on these values, the range of changes for each design parameter was determined as follows:

57.6 mm	<	Throat length	<	70.4 mm
3.6 mm	<	Throat radius	<	20.0 mm
1.8 mm	<	Nozzle radius	<	8.8 mm
2.7 mm	<	Liquid inlet radius	<	14.4 mm
152°	<	Converging angle	<	170°
170°	<	Diverging angle	<	178°

The constants of the genetic algorithm are set, as shown in Table 2. After 111 optimization points, the design has converged, and the design parameters have been optimized, resulting in the determination of three candidate solutions. The results are shown in Table 3.

Table 2

Constants of the multi-objective genetic algorithm.

The constant parameter	Value
Estimated number of design points	1050
Population size	100
Number of samples per iteration	50
Minimum allowed percentage of Pareto	70
Convergence stability percentage	2
Maximum of iteration	20
Number of selected points after optimization	3

Table 3

Geometry of optimal points and the entrainment of the flare gas.

The geometry parameter	base case	1st point	2nd point	3rd point
Throat length, L_T [mm]	64.0	62.99	58.56	63.48

Throat radius, R_T [mm]	8.0	15.29	16.44	18.88
Nozzle radius, R_N [mm]	4.0	4.26	4.66	6.85
Diverging angle (φ)	168	176.99	177.38	177.63
Converging angle (θ)	175	162.79	165.63	153.24
Liquid inlet radius, R_W [mm]	5.5	14.23	11.33	13.26
entrainment rate [kg/s]	0.002485	0.06340	0.03991	0.03172

Figure 4 illustrates the schematic of the candidate design point compared to that of the base case. The results indicate that increasing the radius of the throat and the angle of the divergent part, as well as decreasing the angle of the converging part, lead to an increase in the absorption rate of the gas. Figures 5 and 6 show the axial velocity of the flare gas and liquid respectively. As depicted in Figure 5, the velocity of the secondary fluid is significantly higher in all candidate points compared to that of the base case. The first design point exhibits a higher velocity than the other candidate points. Moreover, the results presented in Figure 6 confirm that all candidate points enhance the axial velocity of the amine compared to the base state.

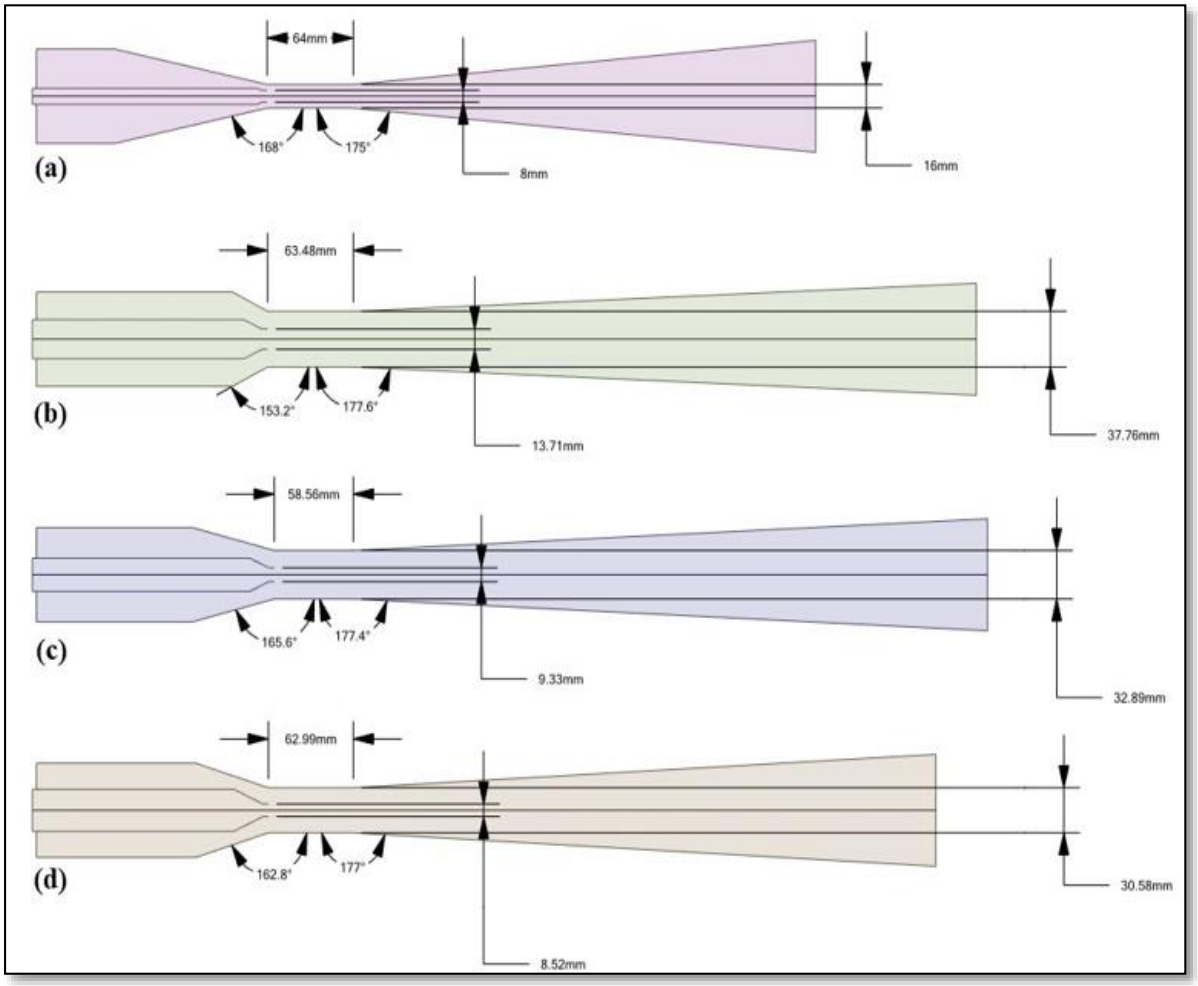

Figure 4. Geometry of three optimal candidates: (a) the base model, (b) the 1st candidate, (c) the 2nd candidate, and (d) the 3rd optimal geometry.

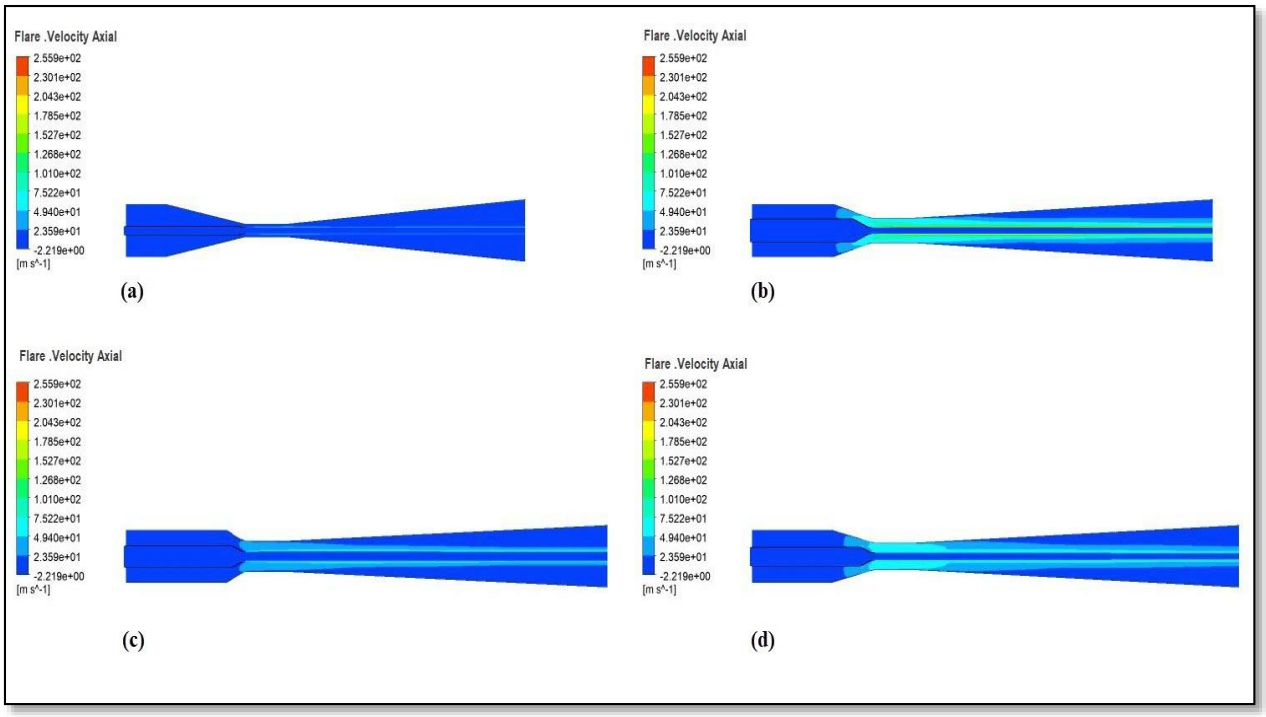

Figure 5. Axial velocity of the flare gas: (a) the base model, (b) the 1st, (c) the 2nd, and (d) the 3rd optimal points.

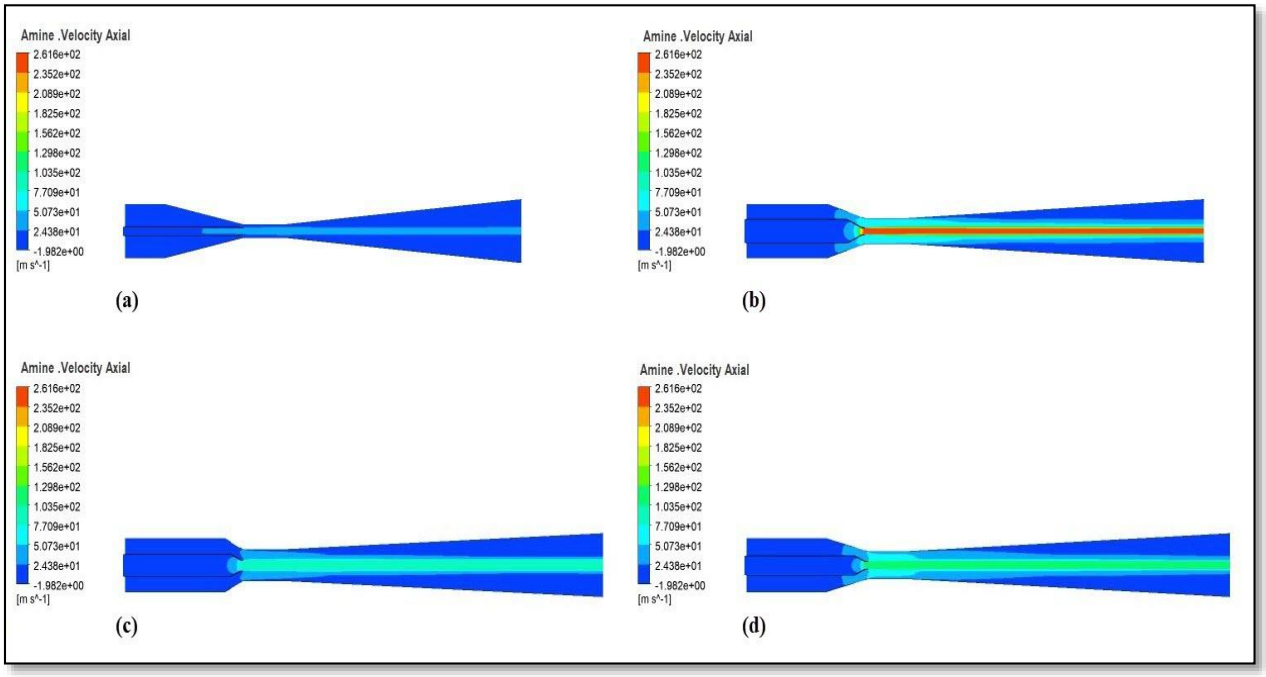

Figure 6. Axial velocity of amine: (a) the base model, (b) the 1st, (c) the 2nd, and (d) the 3rd optimal points.

Among the candidate design points, the first point exhibits a significantly higher axial velocity for the liquid phase compared to the other modes. On the other hand, the second and third design points have the same performance in terms of the axial velocity of the liquid phase. The turbulence intensity of the mixture inside the ejector is depicted in Figure 7, which

shows the base mode and the three design points. The first design point shows a higher turbulence intensity compared to the other two design points. However, the turbulence intensity in the second and third design points is comparable.

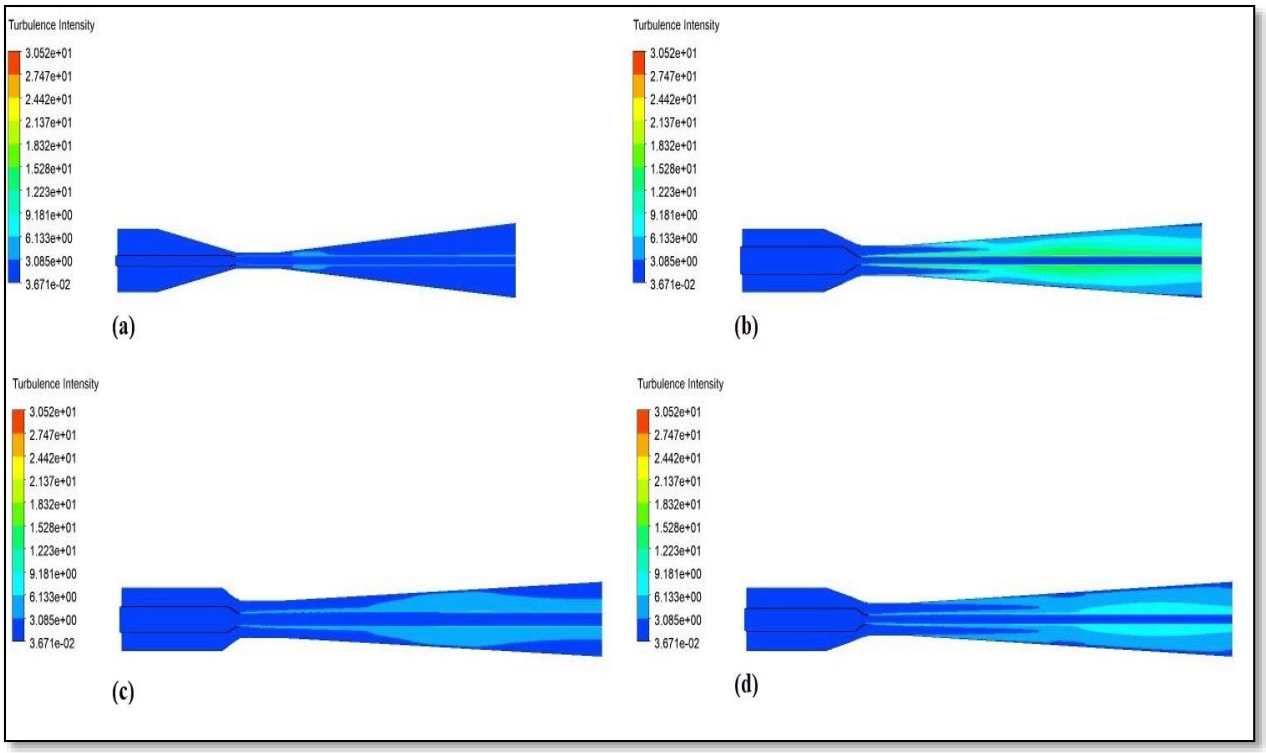

Figure 7. Turbulence intensity of the mixture: (a) the base model, (b) the 1st, (c) the 2nd, and (d) the 3rd optimal points.

5.1. Energy efficiency of the ejector

Based on the obtained results, the first candidate point appears to be the most suitable choice for the ejector design due to its higher axial velocities of both phases and turbulence intensity. However, it is essential to calculate and evaluate the energy efficiency of the ejector as these increases may come at the cost of the higher energy consumption, reducing productivity. The energy efficiency of the ejector can be calculated using the following equation [37].

$$\eta = \left(\frac{\dot{m}_g}{\dot{m}_l}\right)\left(\frac{\Delta P_g}{\Delta P_l}\right) \tag{7}$$

where ΔP_g represents the gas recovery pressure from the suction to the diffuser outlet, and ΔP_l is the liquid pressure drop from the nozzle outlet to the output of the ejector, measured in pascals. The parameters $\dot{m}_g$ and $\dot{m}_l$ represent the flow rate of the gas and the liquid respectively, and they are measured in cubic meters per second.

The efficiency of the ejector was calculated using equation (7) for the base model and the three design points, and the results are presented in Table 4. The second design point exhibited the highest energy efficiency, with an improvement of approximately 3.5 times compared to the base model. The first design point can increase the ejector efficiency up to 78 percent. In contrast, the third design point decreased the energy efficiency by 47 percent.

Table 4
Ejector efficiencies of the three optimal points compared to the base case.

	The base case	Optimal Point		
		1st	2nd	3rd
The energy efficiency	17.79	31.73	60.21	9.40
percentage of change		+78.36 %	+238.42 %	-47.16 %

6. Conclusions

This study investigated a two-phase ejector (liquid-gas) and employed the Euler-Euler approach and mixed method to simulate it. Then, the flow of two-phase fluids was modeled using the Fluent software. The "Coupled" and "PRESTO" models were used for the pressure-velocity connection and discrete pressures, while a second-order upwind model was used for the turbulent kinetic energy, discrete momentum, and rate perturbation loss. The domain was gridded using a structured quadrilateral grid. Different grid sizes were achieved due to the disparity in the results of computational fluid dynamics simulations. In the current study, a numerical solution was obtained using a 0.25 mm grid, resulting in better convergence and fewer fluctuations in the results. The "Realizable" method was used to model the turbulent flow in this research. The considered primary and secondary fluids were amine and the flare gas respectively. The primary aim of this study is to design the geometry of the ejector that maximizes the absorption of the flare gas. To achieve this goal, several design parameters must be optimized, including the length and diameter of the throat, nozzle diameter, liquid inlet diameter, and converging and diverging section angles. In order to define the target variables (i.e., the addition rate) and design, the researchers employed the Fluent software and parametric analysis. To optimize the geometry of the ejector, a multi-objective genetic algorithm was utilized. After reaching 111 points in the convergent design stage, three candidate points were identified where the absorption rate of the flare gas exceeded that of the base case. The optimization process revealed that decreasing the length of the throat and the angle of the converging section resulted in an increased absorption rate of the secondary fluid. Additionally, increasing the nozzle diameter led to an increase in the throat diameter and the angle of the divergent section, resulting in a higher gas absorption rate. The design outcomes yielded the absorption rates for the secondary fluid of 25.5, 16.06, and 12.76 times, compared to that of the base case. The energy efficiency of the ejector was calculated for the base model and all design points. The second design point exhibited the best performance, improving the energy efficiency by approximately 3.5 times compared to the base case. The first design point demonstrated potential for improving the energy efficiency by up to 78 %, whereas the third candidate resulted in a 47 % decrease in the energy efficiency.

Acknowledgement

This manuscript is prepared based on the Ph. D. thesis of the first author at the Islamic Azad University, Borujerd Branch, Borujerd, Iran.

Nomenclature

$\vec{a}$	acceleration vector.
F_d	the drag force [N].
g	gravitational acceleration [m/s^2].
L_T	throat length [mm].
$\dot{m}_g$	gas flow rate [kg/s].

$\dot{m}_l$	fluid flow rate [kg/s].
M_k	forces measurements containing lift, drag, turbulent dispersion, wall lubrication, and virtual mass [N].
p_k	pressure of the phase k [Pa].
ΔP_g	the gas recovery pressure over suction to the diffuser outlet [Pa].
ΔP_l	the liquid pressure drop from the nozzle outlet to the ejector [Pa].
R_T	throat radius [mm].
R_N	nozzle radius [mm].
R_W	liquid inlet radius [mm].
Re	the Reynolds number.
S_k	the rate phase production between different phases.
t_s	relaxation time of secondary phase [s].
u_k	velocity of the phase k [m/s].
α_k	volume fraction of the phase k.
η	the ejector energy efficiency.
ρ_k	density of the phase k [kg/m^3].
μ_k	viscosity of the phase k [Pa.s].
φ	diverging angle [degree].
θ	converging angle [degree].

References

[1] Emam, E. A., "Gas flaring in industry: An overview", *Petroleum & Coal*, **57** (5), 532 (2015).

[2] Soltanieh, M., Zohrabian, A., Gholipour, M. J. and Kalnay, E., "A review of global gas flaring and venting and impact on the environment: Case study of Iran", *International Journal of Greenhouse Gas Control*, **49**, 488 (2016).

[3] Davoudi, M., Rahimpour, M. R., Jokar, S. M., Nikbakht, F. and Abbasfard, H., "The major sources of gas flaring and air contamination in the natural gas processing plants: A case study", *Journal of Natural Gas Science and Engineering*, **13**, 7 (2013).

[4] Elhagar, M., El-Emam, N., Awad, M., Ahmed, A. Z. and Aboul-Fotouh, T. M., "Increase flared gas recovery and emission reduction by separator optimization", *International Journal of Energy and Environmental Engineering*, **12** (1), 115 (2021).

[5] Rahimpour, M., Jamshidnejad, Z., Jokar, S., Karimi, G., Ghorbani, A. and Mohammadi, A., "A comparative study of three different methods for flare gas recovery of Asalooye Gas Refinery", *Journal of Natural Gas Science and Engineering*, **4**, 17 (2012).

[6] Sangsaraki, M. E. and Anajafi, E., "Design criteria and simulation of flare gas recovery system", Proceedings of *the International Conference on Chemical, Food and Environment Engineering (ICCFEE'15*), Dubai, UAE, **15**, 11 (2015).

[7] Zolfaghari, M., Pirouzfar, V. and Sakhaeinia, H., "Technical characterization and economic evaluation of recovery of flare gas in various gas-processing plants", *Energy*, **124**, 481 (2017).

[8] Hajizadeh, A., Mohamadi-Baghmolaei, M., Azin, R., Osfouri, S. and Heydari, I., "Technical and economic evaluation of flare gas recovery in a giant gas refinery", *Chemical Engineering Research and Design*, **131**, 506 (2018).

[9] Hamidzadeh, Z., Sattari, S., Soltanieh, M. and Vatani, A., "Development of a multi-objective decision-making model to recover flare gases in a multi flare gases zone", *Energy*, **203**, 117815 (2020).

[10] Mousavi, S. M., Lari, K., Salehi, G. and Torabi Azad, M., "Technical, economic, and environmental assessment of flare gas recovery system: A case study", *Energy Sources, Part A: Recovery, Utilization, and Environmental Effects*, **9** (1),1 (2020).

[11] Xue, M., Li, X., Cui, X., Cheng, X., Liu, S., Xu, W. and Wang, Y., "A pilot demonstration of flaring gas recovery during shale gas well completion in

china", *SPE Prod. & Oper.*, **38** (3), 504 (2023).

[12] Khalili-Garakani, A., Nezhadfard, M. and Iravaninia, M., "Enviro-economic investigation of various flare gas recovery and utilization technologies in upstream and downstream of oil and gas industries", *Journal of Cleaner Production*, **346**, 131218 (2022).

[13] Zaresharif, M., Vatani, A. and Ghasemian, M., "Evaluation of different flare gas recovery alternatives with exergy and exergoeconomic analyses", *Arabian Journal for Science and Engineering*, **47**, 1 (2021).

[14] Leagas, T., Seefeldt, G. and Hoon, D., "Ejector technology for efficient and cost effective flare gas recovery", Proceedings of *GPA-GCC 24th Annual Technical Conference*, Kuwait City [online], (2016).

[15] Ainge, P., "Ejector technology for flare gas recovery as an alternative to rotating equipment", Proceedings of *Abu Dhabi International Petroleum Exhibition & Conference (SPE)*, (2019).

[16] Mazumder, M., Chen, L. and Xu, Q., "Integrated ejector-based flare gas recovery and on-site desalination of produced water in Shale gas production", *Chemical Engineering & Technology*, **43** (2), 200 (2020).

[17] Eshaghi, S. and Hamrang, F., "An innovative techno-economic analysis for the selection of an integrated ejector system in the flare gas recovery of a refinery plant", *Energy*, **228**, 120594 (2021).

[18] Bashiri, H., Ashrafi, O. and Navarri, P., "Energy-efficient process designs of integrated biomass-derived syngas purification processes via waste heat recovery and integration of ejector technology", *International Journal of Greenhouse Gas Control*, **106**, 103259 (2021).

[19] Ainge, P. and Al-Khateeb, E., "Selection and evaluation of ejectors for flare gas recovery and upstream/midstream gas compression applications", Proceedings of *International Petroleum Technology Conference*, (2022).

[20] Galanis, N. and Sorin, M., "Ejector design and performance prediction", *International Journal of Thermal Sciences*, **104**, 315 (2016).

[21] Wang, L., Yan, J., Wang, C. and Li, X., "Numerical study on optimization of ejector primary nozzle geometries", *International Journal of Refrigeration*, **76**, 219 (2017).

[22] Śmierciew, K., Gagan, J. and Butrymowicz, D., "Application of numerical modelling for design and improvement of performance of gas ejector", *Applied Thermal Engineering*, **149**, 85 (2019).

[23] Suvarnakuta, N., Pianthong, K., Sriveerakul, T. and Seehanam, W., "Performance analysis of a two-stage ejector in an ejector refrigeration system using computational fluid dynamics", *Engineering Applications of Computational Fluid Mechanics*, **14** (1), 669 (2020).

[24] Li, H., Wang, X., Ning, J., Zhang, P., Huang, H. and Tu, J., "Numerical investigation of the nozzle expansion state and its effect on the performance of the steam ejector based on ideal gas model", *Applied Thermal Engineering*, **199**, 117509 (2021).

[25] Xu, J., Liu, X. and Pang, M., "Numerical and experimental studies on transport properties of powder ejector based on

double venturi effect", *Vacuum*, **134**, 92 (2016).

[26] Sriveerakul, T., Aphornratana, S. and Chunnanond, K., "Performance prediction of steam ejector using computational fluid dynamics: Part 1, Validation of the CFD results", *International Journal of Thermal Sciences*, **46** (8), 812 (2007).

[27] Yadav, R. L. and Patwardhan, A. W., "Design aspects of ejectors: Effects of suction chamber geometry", *Chemical Engineering Science*, **63** (15), (2008).

[28] Ariyaratne, W. H., Manjula, E. V. P. J., Ratnayake, C. and Melaaen, M. C., "CFD approaches for modeling gas-solids multiphase flows–A review", Proceedings of *9th EUROSIM, The 57th SIMS Conference on Simulation and Modelling SIMS 2016*, Linköping University Electronic Press, **142**, 680 (2018).

[29] Suh, J. W., Kim, J. W., Choi, Y. S., Kim, J. H., Joo, W. G. and Lee, K. Y., "Development of numerical Eulerian-Eulerian models for simulating multiphase pumps", *Journal of Petroleum Science and Engineering*, **162**, 588 (2018).

[30] Song, X., Cao, M., Shin, W., Cao, W., Kang, S. and Park, Y., "Numerical investigation of a liquid-gas ejector used for shipping ballast water treatment", *Mathematical Problems in Engineering*, (2014).

[31] Alshebani, M. E., Alawadhi., K., Alnaqi, A. A. and Saker, A. A., "Numerical investigation of a liquid-gas ejector in marine ships", *International Journal of Applied Engineering Research*, **12** (14), 4663 (2017).

[32] Parekh, J. and Rzehak, R., "Euler–Euler multiphase CFD-simulation with full Reynolds stress model and anisotropic bubble-induced turbulence", *International Journal of Multiphase Flow*, **99**, 231 (2018).

[33] Kwiatoń, P., Cekus, D., Miara, M. and Kubik-Maciąg, I., "Multiphase modeling of droplet fall using Euler-Euler approach", *Acta Physica Polonica A*, **138** (2), 276 (2020).

[34] Frank, T., Zwart, P., Krepper, E., Prasser, H. M. and Lucas, D., "Validation of CFD models for mono-and polydisperse air–water two-phase flows in pipes", *Nuclear Engineering and Design*, **238** (3), 647 (2008).

[35] Selvakumar, R. D. and Dhinakaran, S., "Forced convective heat transfer of nanofluids around a circular bluff body with the effects of slip velocity using a multi-phase mixture model", *International Journal of Heat and Mass Transfer*, **106**, 816 (2017).

[36] Manninen, M., Taivassalo, V. and Kallio, S., "On the mixture model for multiphase flow", Technical Research Center of Finland, VTT Publications, (1996).

[37] Bhutada, S. and Pangarkar, V., "Gas induction and hold-up characteristics of liquid jet loop reactors", *Chemical Engineering Communications*, **61** (1-6), 239 (1987).

[38] Ringstad, K. E., Allouche, Y., Gullo, P., Ervik, Å., Banasiak, K. and Hafner, A., "A detailed review on CO_2 two-phase ejector flow modeling", *Thermal Science and Engineering Progress*, **20**, 100647 (2020).

[39] De Oliveira Marum, V. J., Reis, L. B., Maffei, F. S., Ranjbarzadeh, S., Korkischko, I., dos Santos Gioria, R. and Meneghini, J. R., "Performance analysis of a water ejector using Computational

Fluid Dynamics (CFD) simulations and mathematical modeling", *Energy*, **220**, 119779 (2021).

[40] Zolpakar, N. A., Lodhi, S. S., Pathak, S. and Sharma, M. A., "Application of multi-objective genetic algorithm (MOGA) optimization in machining processes", Optimization of Manufacturing Processes, Springer, p. 1-15 (2020).

[41] Murata, T. and Ishibuchi, H., "MOGA: multi-objective genetic algorithms", Proceedings of *IEEE International Conference on Evolutionary Computation*, NJ, USA, (1995).

[42] Deb, K., "Multi-objective genetic algorithms: Problem difficulties and construction of test problems", *Evolutionary Computation*, **7** (3), 205 (1999).